

Mechanical properties and deformation behavior of carbon nanotubes calculated by a molecular mechanics approach

Oliver Eberhardt* and Thomas Wallmersperger

Institut für Festkörpermechanik, Technische Universität Dresden, George-Bähr-Straße 3c, 01069 Dresden, Germany

(Received April 9, 2013, Revised November 25, 2013, Accepted November 30, 2013)

Abstract. Carbon nanotubes are due to their outstanding mechanical properties destined for a wide range of possible applications. Since the knowledge of the material behavior is vital regarding the possible applications, experimental and theoretical studies have been conducted to investigate the properties of this promising material. The aim of the present research is the calculation of mechanical properties and of the mechanical behavior of single wall carbon nanotubes (SWCNTs). The numerical simulation was performed on basis of a molecular mechanics approach. Within this approach two different issues were taken into account: (i) the nanotube geometry and (ii) the modeling of the covalent bond. The nanotube geometry is captured by two different approaches, the roll-up and the exact polyhedral model. The covalent bond is modeled by a structural molecular mechanics approach according to Li and Chou. After a short introduction in the applied modeling techniques, the results for the Young's modulus for several SWCNTs are presented and are discussed extensively. The obtained numerical results are compared to results available in literature and show an excellent agreement. Furthermore, deviations in the geometry stemming from the different models are given and the resulting differences in the numerical findings are shown. Within the investigation of the deformation mechanisms occurring in SWCNTs, the basic contributions of each individual covalent bond are considered. The presented results of this decomposition provide a deeper understanding of the governing deformation mechanisms in SWCNTs.

Keywords: carbon nanotube; single wall nanotube; molecular mechanics; mechanical properties; modeling

1. Introduction

1.1 General properties

The interest on carbon based nano materials originated from the discoveries made by Iijima (1991), who observed that carbon nanotubes are produced during arc discharge between carbon electrodes. It has to be noted that the actual discovery of carbon nanotubes was made by the soviet scientists Radushkevich and Lukyanovich (1952). During their carbon-related research, they found carbon nanotubes with diameters of around 50 nm. However, it was the work of Iijima which was the ignition for the fast-growing interest in carbon nanotube research, since he delivered two

*Corresponding author, Ph.D. Student, E-mail: Oliver.Eberhardt@tu-dresden.de

important contributions regarding the understanding of carbon nanotubes. These contributions are (i) the conclusion that carbon nanotubes are produced during arc discharge (Iijima (1991)), and (ii) the attempt to fill carbon nanotubes with metals, which resulted in the production of single wall carbon nanotubes (Iijima and Ichihashi (1993)).

A single wall carbon nanotube can be imagined as a cut-out of a layer of graphene which is rolled up into a seamless tube. Hence, carbon nanotubes show the same hexagonal structure as graphene does. The reason for the numerous research efforts are the predicted outstanding mechanical (e.g., see Treacy *et al.* (1996)), electrical (e.g., see Tans *et al.* (1997)) and thermal (e.g., see Berber *et al.* (2000)) properties of the carbon nanotubes. Hence, numerous ideas for applications in many fields of engineering and science have been proposed. The present research focuses on the mechanical behavior of the carbon nanotubes; a possible application in this field could be their use as reinforcing material in composites. This can be done for example by simply adding a particular amount of carbon nanotubes into the matrix material. A review concerning this kind of carbon nanotube composites can be found in Thostenson *et al.* (2001). Another possibility is the use of fibers spun from carbon nanotubes, which are discussed as possible successors of the widely used carbon fibers. A review on the current state of research in the technology of carbon nanotube fibers was given recently by Lu *et al.* (2012). Regarding the electro-mechanical behavior it was found that carbon nanotubes respond to electrical fields with an active deformation. Baughman *et al.* (1999) realized a carbon nanotube actuator based on bucky paper submerged in a liquid electrolyte. Bucky paper can be described as a kind of felt made from carbon nanotubes. The actuation mechanism (expansion) is based on an electrochemical double-layer charging. Carbon nanotube fibers have also been recently proposed by Foroughi *et al.* (2011) as torsional actuators. Furthermore, individual nanotubes respond to electrical stimulation as well, and can hopefully be used as actuators on the nanoscale. Regarding an individual carbon nanotube actuator, the extension of the nanotube is a result of charge injection in the carbon nanotube structure which leads to an extension of the covalent bonds within the carbon nanotube.

The outstanding mechanical properties mentioned above include a remarkably high Young's modulus and excellent strength. Values of around 1 TPa for the Young's modulus have been found with theoretical approaches, e.g., Tserpes and Papanikos (2005), and experimental studies, e.g., Wu *et al.* (2008). Regardless if a theoretical or experimental approach is chosen, the determination of these properties poses several challenges which will be discussed within the present research.

1.2 Modeling

During the past years, several methods regarding the calculation of the mechanical properties of carbon nanotubes have been proposed. Due to the size of the nanotubes, the question arises to what extent quantum mechanical models have to be used, or whether classical models are applicable. Therefore the approaches made so far can be divided into quantum-mechanical methods and methods stemming from classical mechanics. As examples for quantum-mechanical approaches the works of Hernández *et al.* (1998), Sánchez-Portal *et al.* (1999), Kudin *et al.* (2001), and more recently Chandraseker and Mukherjee (2007) should be mentioned. Chandraseker and Mukherjee (2007) used a density-functional-theory (DFT) approach to calculate the Young's modulus and the shear modulus. Furthermore, they used a classical approach to calculate these properties in order to compare the results gained with these two different methods. In the group of classical mechanics methods one can find on the one hand approaches which model the nanotubes as a continuum, while on the other hand atomistic approaches, for instance based on molecular

mechanics, are available.

In their continuum approach Odegard *et al.* (2002) developed an equivalent continuum model based on plates. Cinefra *et al.* (2011) used a refined shell model based on Carrera's Unified Formulation to investigate the free vibration response of double wall carbon nanotubes.

Some of the molecular mechanics models make use of the Finite Element Method framework, e.g., Li and Chou (2003), Tserpes and Papanikos (2005), Meo and Rossi (2006) and Giannopoulos *et al.* (2008). All these researchers aimed at the determination of mechanical properties of single wall carbon nanotubes. While Li and Chou (2003) and Tserpes and Papanikos (2005) applied truss-beam elements to model the covalent bonds in the carbon nanotubes, the models of Meo and Rossi (2006) and Giannopoulos *et al.* (2008) used combinations of spring elements. The approach of the present work is based on molecular mechanics and uses truss-beam elements. As a result the nanotube geometry and the material behavior of the covalent bonds in the carbon nanotubes can be treated separately.

In order to get better results for the radial elasticity and the Poisson's ratio, Chen *et al.* (2010) extended the molecular mechanics model of Li and Chou (2003). As in the original model, they used truss-beam elements, but extended the existing theory to account for a non-circular cross section.

1.3 Outline of the present work

The present work is structured as follows: A brief description of carbon nanotubes is given in section 2. The general structure of carbon nanotubes is illustrated and the existing types of carbon nanotubes are distinguished. On the basis of these types the construction of the unit cell as the basic construction element of the carbon nanotubes is explained.

The description of the applied models is given in section 3. The general overview of the model clarifies why the modeling can be divided into two parts which are (i) the representation of the nanotube geometry and (ii) the model of the covalent bond. Concerning the nanotube geometry, two different models are used in the present research, and are illustrated in section 3.1. These are on the one hand the roll-up model and on the other hand the exact polyhedral model developed by Cox and Hill (2007). The comparison of these two geometric models is one important topic of the present research. The approach to model the covalent bonds in the nanotubes is based on the works of Li and Chou (2003) and Tserpes and Papanikos (2005), and is summarized in section 3.2.

Section 4 presents the results of the numerical simulations based on the described modeling techniques. The major goal of this study is the determination of the mechanical properties and of the mechanical behavior of single wall carbon nanotubes. Hence, the Young's modulus for several single wall carbon nanotubes of different types with various diameters is computed on the basis of a virtual tensile test. These results are compared to results available in literature. As a special feature of the present research, these mechanical properties are calculated based on the two different geometrical models explained above. The numerically obtained deviations are analyzed by closely observing the nanotube geometry which is determined by the bond length and the bond angle.

Another focus of this work is formed by the investigation of the deformation behavior of single wall carbon nanotubes. To do this, the carbon nanotubes are subjected to a tensile force which results in an extension of the carbon nanotube. This deformation is then subdivided into the contributions stemming from covalent bond deformations. Hence, this approach grants a

deeper insight into the mechanical behavior of carbon nanotubes.

In the conclusion (Section 5), the results of the numerical investigations are summarized.

2. Brief description of carbon nanotubes

As already mentioned, one can imagine the carbon nanotube as a layer of graphene which is rolled up into a seamless tube. As a result, the carbon nanotube shows a hexagonal structure comparable to that of graphene, where one carbon atom is located at each edge of the hexagons. Due to the sp^2 - hybridization of the carbon atoms, each carbon atom is connected to its three neighbors via covalent bonds. One can distinguish between single and multi wall carbon nanotubes (SWCNT/MWCNT). As the name states, the SWCNTs are made out of a single graphene layer, while MWCNTs are numerous SWCNTs stacked together on a common axis. Furthermore, one can distinguish between three SWCNT subtypes called the

- armchair
- zig-zag
- chiral

type. These SWCNTs can be derived from different unit cells. The unit cell is constructed as a cut-out of a graphene layer which is rolled up into a tube. To describe this cut-out, a chiral vector $\underline{\mathbf{C}}$ and a translational vector $\underline{\mathbf{T}}$ have to be defined. Additionally, in literature, e.g., in Dresselhaus *et al.* (1995), often a chiral angle θ is given, see Fig. 1.

The unit cell is uniquely defined by a pair of two integers (n, m) which specify the chiral vector with respect to the coordinate system given by the basis vectors $\underline{\mathbf{a}}_1$ and $\underline{\mathbf{a}}_2$. With the knowledge of the chiral vector $\underline{\mathbf{C}}$ one can calculate the translational vector $\underline{\mathbf{T}}$. Now, the cut-out of the graphene layer can be rolled up in the direction of $\underline{\mathbf{C}}$. For more details concerning the geometrical nanotube properties and how to calculate the translational vector, the interested reader is referred to the work by Dresselhaus *et al.* (1995).

Fig. 1 shows how the unit cells for different types of SWCNTs are constructed. Based on this figure it is possible to reproduce the calculation of the chiral vector $\underline{\mathbf{C}}$ on the basis of the associated index pairs. For armchair SWCNTs the translational vector is always given as $\underline{\mathbf{T}} = (-1, 1)$ while for zig-zag tubes it is $\underline{\mathbf{T}} = (-1, 2)$. For chiral SWCNTs the translational vector has to be calculated according to Dresselhaus *et al.* (1995).

3. Modeling approach

As a starting point, the carbon nanotube is given in its chemical representation with the carbon atoms and the covalent bonds, see Fig. 2. The behavior of the bonds can be described by a chemical force field representation. A chemical force field is applied in computational chemistry for instance for the conformational analysis of molecules. For that purpose, various parameters are used. These parameters are named chemical force constants k_r , k_θ , k_τ , see Fig. 2. More details on the application and the origin of these constants are given in section 3.2. The goal of the present research is a mechanical representation of the carbon nanotubes based on the given chemical description. Since the mechanical properties are of interest, a transfer of the chemical model into a mechanical model has to be gained, see Fig. 2.

The modeling approach can be divided into two parts which can be considered independently of each other. These two parts are (i) the nanotube geometry and (ii) the representation of the covalent bond. The first thing to consider is the nanotube geometry which is basically given by the position of the carbon atoms in the nanotube. In this work two different geometrical models have been used and compared, see section 3.1.

Secondly, a proper representation for the covalent bond needs to be found. The approach which was applied here is the molecular structural mechanics (MSM) approach as it was first suggested by Li and Chou (2003) with extensions made by Tserpes and Papanikos (2005), see section 3.2.

These efforts aim on the determination of the global mechanical properties of single wall carbon nanotubes.

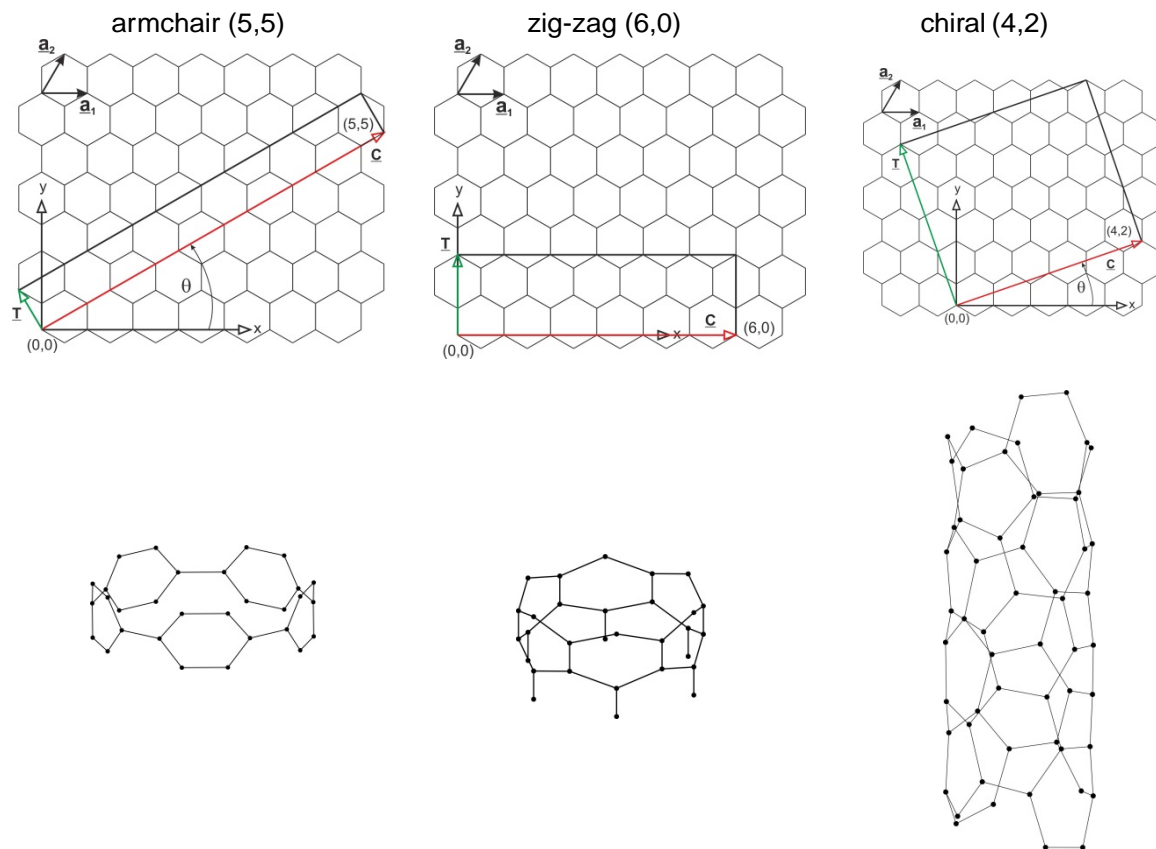


Fig. 1 Schematic representation of the construction of a unit cell for armchair, zig-zag and chiral nanotubes. The chiral vector \underline{C} is given as red colored arrow, while the translational vector \underline{T} is green colored. The pictures below the construction sketches show a three-dimensional view of the constructed unit cells

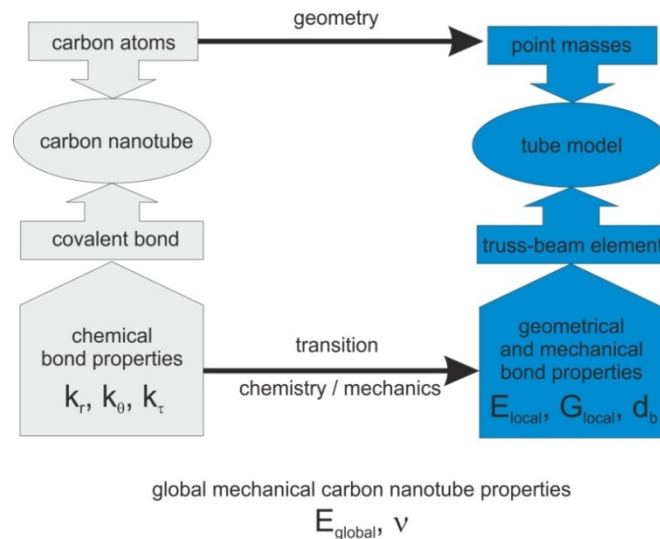


Fig. 2 Modeling approach, schematic representation

3.1 Geometric models

The geometry deals with the position of the carbon atoms in the nanotube. For dynamic investigations, the atoms could be modeled as point masses. However, since the present research only includes static numerical simulations, the carbon atoms are simply represented as nodes where the covalent bonds are connected. In the present research two different geometric models are compared. These are the roll-up and the exact polyhedral model.

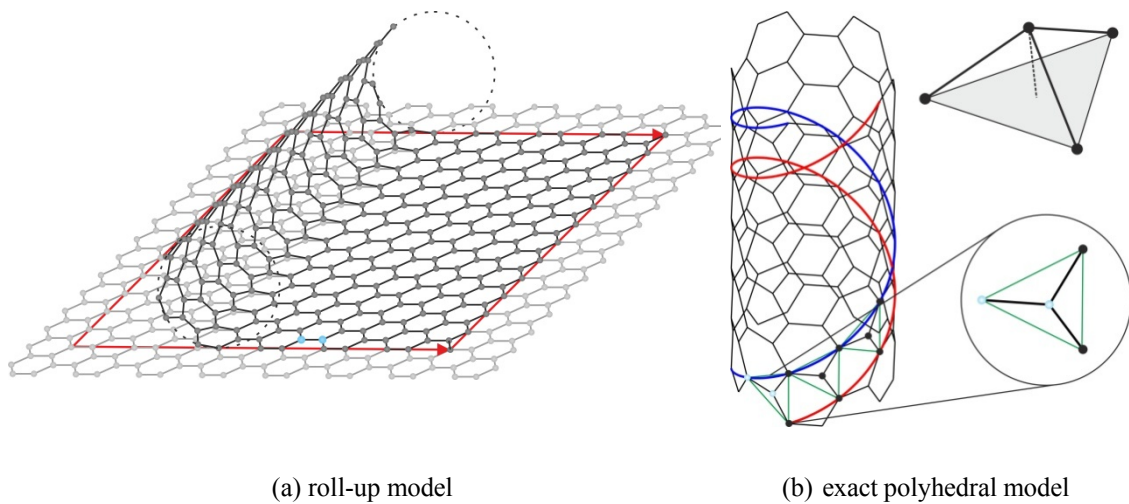
The roll-up model, see Fig. 3(a), is commonly used. It stems from the idea of using a rolled up cut-out in a graphene layer as already discussed in section 2. The disadvantage of this model is that curvature effects result in unequal bond lengths in the nanotube. This error decreases for increasing nanotube diameters.

The other presented model, the exact-polyhedral model, was proposed by Cox and Hill (2007) in order to create a geometric model in which all bonds are of the same specific length, see Fig. 3(b). It uses tetrahedrons placed on helices to fulfill this condition. The tetrahedrons are subjected to a special transformation which changes the position and orientation of the tetrahedrons in space depending on the chirality (n, m) of the tube being constructed.

Fig. 4 reveals the error made with the roll-up model. For example, the transformation during the roll-up of a covalent bond perpendicular to the nanotube axis is observed, see the bond between the blue colored atoms in Fig. 3(a). Prior to the roll-up of the graphene sheet, the length between the two atoms is equal to one bond length a_{C-C} . Due to the roll-up in the marked direction, it is obvious, that the once straight connection between the atoms is transformed into the red-colored circular arc given in Fig. 4 (right). The length of this arc is a_{C-C} . However, in the nanotube the direct connection - instead of the arc - between these atoms has to be identical to one bond length a_{C-C} . From these considerations it can be deduced that in the roll-up model the direct connection between the investigated atoms is too short. This effect can be observed for all bonds which are not

parallel to the nanotube axis.

Owing to the special approach of the exact polyhedral model, this problem doesn't occur there. The exact polyhedral model yields the correct bond length as shortest connection between the two considered atoms, see Fig. 4 (right). For details regarding this geometric model see Cox and Hill (2007).



(a) roll-up model

(b) exact polyhedral model

Fig. 3 Geometric models used in this paper

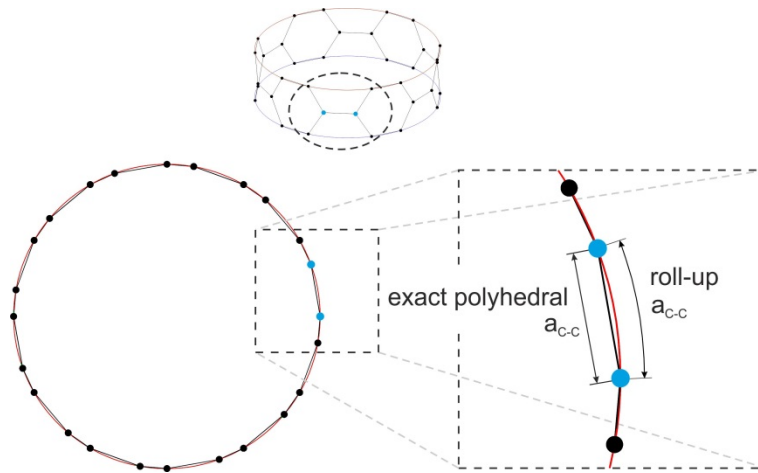


Fig. 4 Schematic representation of the resulting error due to the improperly considered curvature of the nanotube as it arises when using the roll-up model. For comparison purposes the correct bond length as calculated by the exact polyhedral model according to Cox and Hill (2007) is also depicted

3.2 Representation of the covalent bond

After describing the modeling of the geometry (section 3.1), it is necessary to take the modeling of the covalent bond in SWCNTs into account, see Fig. 2. The bond is modeled in this research with the molecular structural mechanics approach according to Li and Chou (2003) and Tserpes and Papanikos (2005). An overview of the applied method is given in this section of the paper.

As already mentioned, the starting point of the modeling efforts is a chemical force field description characterizing the covalent bond with help of the chemical force constants k_r , k_θ and k_τ . To transfer this chemical representation into a mechanically applicable representation, the molecular structural mechanics approach is applied. In this approach the covalent bond is represented by a (Euler-Bernoulli) truss-beam element with six degrees of freedom (three translational u_x , u_y , u_z and three rotational ϕ_x , ϕ_y , ϕ_z degrees of freedom per node) at each node. As a result, it is necessary to compute all the properties for the beam material as well as the beam geometry from the chemical force field description. The properties of the beam and its material which have to be computed are:

- the Young's modulus E of the truss-beam element describing the covalent bond,
- the shear modulus G of the truss-beam element describing the covalent bond,
- the diameter d of the truss-beam element, when a circular cross section of the truss-beam element representing the bond is assumed,
- the length l of the truss-beam element.

The chemical force field description allows the calculation of an overall potential U which describes the conformation of the analyzed structure and also describes changes in the conformation (deformation) when the structure is subjected to loads. The overall potential U is assembled from several contributions stemming from the possible deformations of each single bond in the investigated structure. Additionally, van-der-Waals and electrostatic interactions have to be taken into account. The possible bond deformations include (see also Fig. 5):

- bond stretching,
- bond angle bending,
- bond torsion and
- inversion or out-of-plane torsion.

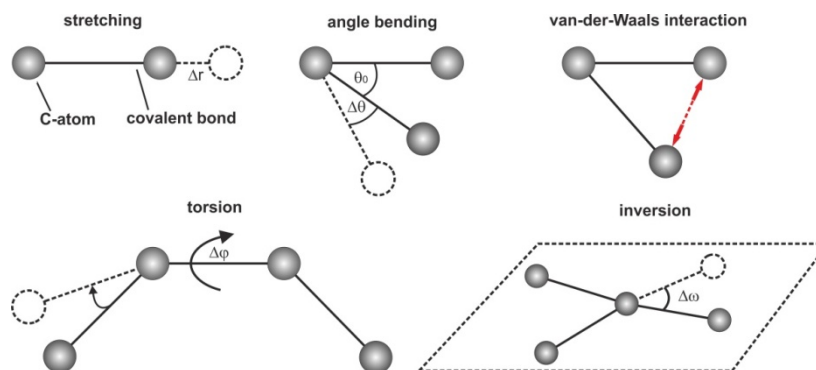


Fig. 5 Possible bond deformations of a single covalent bond

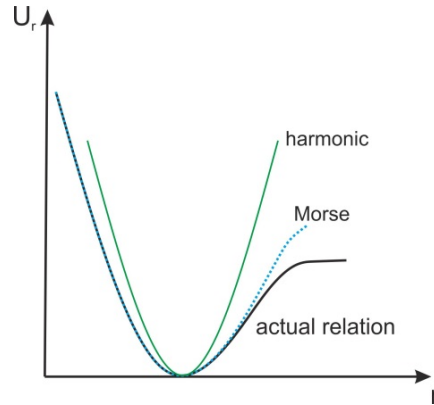


Fig. 6 Bond stretch potential measured versus the bond length r . Actual relation and approximations

Due to these bond deformations, van-der-Waals and electrostatic interactions the overall potential U reads

$$U = \underbrace{\sum U_r}_{\text{stretching}} + \underbrace{\sum U_\theta}_{\text{angle bending}} + \underbrace{\sum U_\varphi}_{\text{torsion}} + \underbrace{\sum U_\omega}_{\text{inversion}} + \underbrace{\sum U_{vdW}}_{\text{van-der-Waals}} + \underbrace{\sum U_{el}}_{\text{electrostatic}} \quad (1)$$

For the modeling of SWCNTs as it is done in this paper, the van-der-Waals and electrostatic interactions are not taken into account. For the sake of completeness it should be noted here that the van-der-Waals bonds cannot be neglected when MWCNTs are modeled. For the SWCNTs it has to be mentioned that in accordance with the approach of Li and Chou (2003) the inversion potential U_ω and the bond torsion potential U_φ are combined into a single contribution U_τ , so that the overall potential U used within the present research is given by

$$U = \sum U_r + \sum U_\theta + \sum U_\tau \quad (2)$$

One of the major aspects in modeling the covalent bond is the choice of proper potentials for each of these contributions. On the basis of the bond stretch as an example some considerations regarding the potential representation are shown. Fig. 6 shows the actual relationship for the bond stretch potential U_r measured versus the distance between two bonded atoms r . In this figure it can be recognized that the harmonic approximation,

$$U_r = \frac{1}{2} k_r (\Delta r)^2 \quad (3)$$

which makes use of a quadratic function, is only valid for small deformations around the equilibrium bond length. The parameter k_r is the chemical force constant responsible for the bond stretch behavior, and Δr is the change in the distance of the two bonded atoms. Another possibility is the application of the Morse-Potential which was used in the work of Meo and Rossi (2006)

$$U_r = D_e \left(1 - e^{-\beta \Delta r}\right)^2 \quad (4)$$

This has the disadvantage that it comes with a higher numerical effort. In this equation D_e and β are parameters which have to be chosen in accordance with the covalent bond being modeled. Depending on the chemical element of the connected atoms, different values for the parameters have to be used. Since our investigations only consider small deformations so far, the use of harmonic approximations is adequate. This type of potential is not only applied for the bond stretching, but also for the bond angle bending and the bond torsion. The above-mentioned combination of the bond torsion and inversion potentials follows the idea of Li and Chou (2003). This combination is done by adding the corresponding chemical force constants. Hence, the potentials read as follows

$$U_r = \frac{1}{2} k_r (\Delta r)^2 \quad (5)$$

$$U_\theta = \frac{1}{2} k_\theta (\Delta \theta)^2 \quad (6)$$

$$U_\tau = \frac{1}{2} (k_\phi + k_\omega) (\Delta \phi)^2 = \frac{1}{2} k_\tau (\Delta \phi)^2 \quad (7)$$

In these equations k_r , k_θ , k_ϕ and k_ω are the chemical force constants responsible for the bond stretching, bond angle bending, bond torsion and bond inversion. The constant k_τ is the result of the addition of k_ϕ and k_ω . The variables Δr , $\Delta \theta$ and $\Delta \phi$ are the extension of the bond, the angle change due to bending as well as the change of the torsional angle. The quantitative values of these chemical force constants are determined in dependence of the chosen chemical force field and furthermore in dependence of the atom type. Here, the atom type is the chemical element of the two connected atoms as well as the specific type of the covalent bond indicated by its hybridization. Hence, for SWCNTs it is necessary to choose force constants which were determined to describe the covalent bond between carbon atoms with sp^2 -hybridization. In this research a force field with chemical force constants according to Cornell *et al.* (1995) is used. Hence, the values of the chemical force constants are

$$k_r = 938 \frac{\text{kcal}}{\text{mol } \text{\AA}^2} = 652.13 \frac{\text{kg}}{\text{s}^2}$$

$$k_\theta = 126 \frac{\text{kcal}}{\text{mol rad}^2} = 87.60 \frac{\text{kg } \text{\AA}^2}{\text{s}^2 \text{ rad}^2}$$

$$k_\tau = 40 \frac{\text{kcal}}{\text{mol rad}^2} = 27.81 \frac{\text{kg } \text{\AA}^2}{\text{s}^2 \text{ rad}^2}$$

where $1 \text{ \AA} = 10^{-10} \text{ m}$.

As next step the chemical representation and the mechanical description, based on a truss-beam element, of the covalent bond are compared regarding its possible deformations. On the basis of the bond-stretching, for example, it can be explained how a bridging between the chemical and the mechanical description can be established, see Fig. 7.

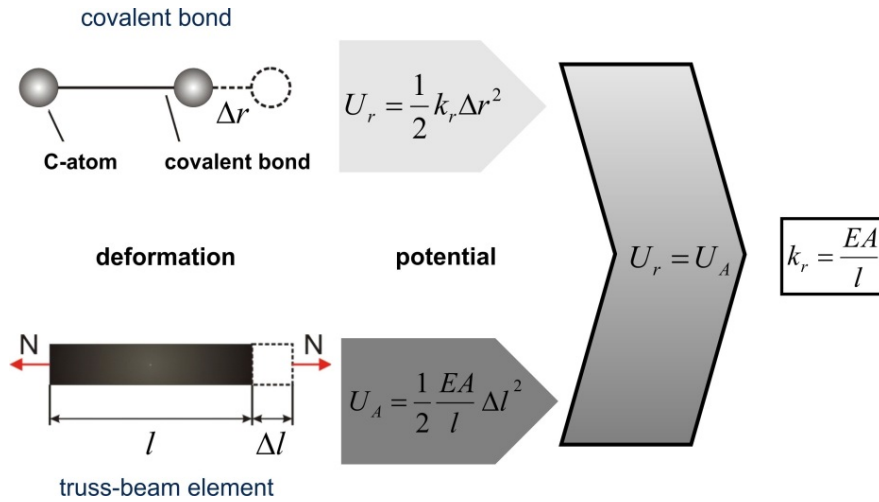


Fig. 7 Comparison of the bond stretching description in the chemical and mechanical representation

In this figure it can be recognized that the stretching of the bond in the chemical representation is equivalent to the stretching of the truss-beam element. Both phenomena can be described via their potentials. On the one hand there is the chemical potential describing the stretching of the covalent bond. On the other hand the stretching of the truss-beam element is described by a mechanical potential which is given as the elastic strain energy. Hence, these two potentials can be equated which yields the desired transfer between the chemical and the mechanical/geometrical properties.

This procedure can be performed in an analogous manner for the bond angle bending and the bond torsion. The result is a set of three equations connecting the chemical properties with the mechanical/geometrical ones

$$k_r = \frac{EA}{l} \tag{8}$$

$$k_\theta = \frac{EI}{l} \tag{9}$$

$$k_\tau = \frac{GJ}{l} \tag{10}$$

These equations contain the material parameters assigned to the covalent bonds, which are the Young's modulus E and the shear modulus G , the cross-sectional area A , the moment of inertia I , the torsional moment of inertia J and the length of the truss-beam element l . When a circular cross section of the bond is assumed, it is possible to determine all parameters of the truss-beam element with the Eqs. (8), (9) and (10) and the properties of the cross section

$$A = \frac{\pi}{4} d_b^2 \quad (11)$$

$$I = \frac{\pi}{64} d_b^4 \quad (12)$$

$$J = \frac{\pi}{32} d_b^4 \quad (13)$$

Here d_b is the diameter of the bond cross section, which should not be mistaken with the global nanotube diameter used later in the present research. The length of the truss-beam element can be identified as the original bond length $a_{C-C} = 1.421 \text{ \AA}$. It has to be mentioned here that this original bond length is used to calculate the truss-beam parameters for all the bonds, also when using the roll-up model which yields improper bond lengths. Hence, the undesired differences in the bond lengths in the roll-up model only have impact on the nanotube geometry. Summarizing, by using Eqs. (8)-(13) the parameters for the covalent bond E , G , d_b and l are obtained

$$E = \frac{k_r^2 l}{4 \pi k_\theta} \quad (14)$$

$$G = \frac{k_r l k_r^2}{8 \pi k_\theta^2} \quad (15)$$

$$d_b = 4 \sqrt{\frac{k_\theta}{k_r}} \quad (16)$$

$$l = a_{C-C} \quad (17)$$

As all the properties required to represent the covalent bond with the truss-beam elements are now defined, this concludes the modeling of the covalent bond.

4. Numerical results of the mechanical properties and deformation behavior

4.1 Young's modulus

One major goal within the carbon nanotube research is the determination of the global mechanical properties of the individual carbon nanotubes and especially of the Young's modulus. As a result of this, a virtual tensile test was conducted in order to calculate this property. This was done by fixing the nanotubes at one end while pulling at the other one with a tensile force resulting in 1% tensile strain of the investigated SWCNT. The application of these boundary conditions is shown in Fig. 8. The study was conducted for several armchair and zig-zag nanotubes with different diameters within the framework of the FE-package ABAQUS.

One has to face several challenges in the calculation of the mechanical properties and especially in the calculation of the Young's modulus. The reasons for these difficulties are due to the assumptions made and also due to the definition of the Young's modulus which requires a scaling with respect to

the cross-sectional area. These assumptions are:

- Linear elastic material behavior of the overall nanotube according to Hooke's law. Since small deformations of the tube are considered, this statement seems reasonable. Furthermore, the applied harmonic potentials also require the assumption of small deformations since they describe a linear material behavior of the bonds within the nanotube.
- A uniform distribution of the tensile stress on the CNT cross section.
- The cross section of the carbon nanotube is a hollow cylinder with a wall thickness t .

These considerations lead to a still ongoing discussion regarding the imagined cross section of the carbon nanotube. The challenge is, that it is not yet explained how a cross section, or, to be more specific, how a wall thickness can be defined for a structure which has a thickness of only one atomic layer. The most commonly used assumption for this wall thickness is the use of the interlayer spacing of graphite which is 0.34 nm. This assumption is also used in this paper, keeping in mind that the topic is still under discussion, see Fig. 9.

It also has to be mentioned here, that these problems not only occur in theoretical but also in experimental studies concerning the mechanical properties of carbon nanotubes. Perhaps it would be better to determine not the Young's modulus but a stiffness (EA) or an elastic spring constant EA/L , with the overall length L of the nanotube, as for the calculation of this stiffness it is not mandatory to define a cross section of the nanotube. However, since the results given in this research should be comparable to results available in literature, this research will state the Young's modulus with respect to the above-mentioned assumptions regarding the nanotube cross section.

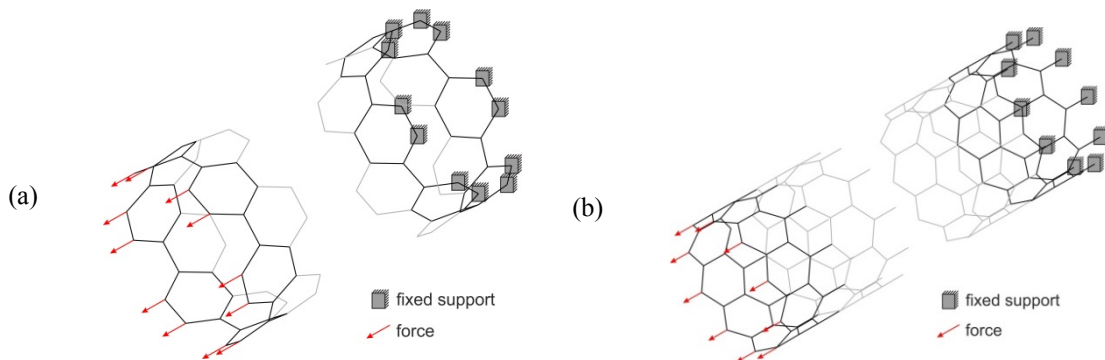


Fig. 8 Schematic representation of the mechanical boundary conditions for armchair (a) and zig-zag (b) nanotubes

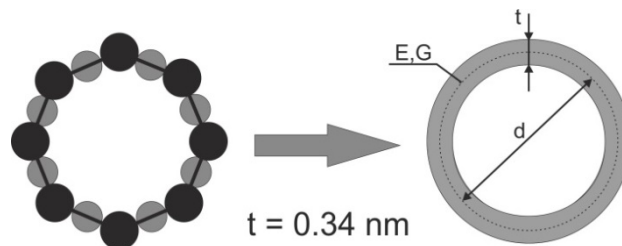


Fig. 9 Virtual cross section assigned to the carbon nanotube

Concerning the calculation of the Young's modulus one has to follow the assumptions given above. The elasticity law for linear elastic material behavior yields

$$\sigma = E \varepsilon \quad (18)$$

where σ , E and ε denote the carbon nanotubes stress, Young's modulus and strain. The strain in longitudinal direction of the tube can be written in dependence of the numerically obtained extension of the nanotube ΔH , and the undeformed investigated nanotube length H

$$\varepsilon = \frac{\Delta H}{H} \quad (19)$$

Furthermore the stress σ can also be written as

$$\sigma = \frac{F}{A} \quad (20)$$

where F is the tensional force the nanotube is subjected to, and A is the cross-sectional area. The cross-sectional area is calculated based on the wall thickness t and the circumference of the nanotube πd by

$$A = \pi d t \quad (21)$$

As a result of this, the nanotube diameter d can be interpreted as the mean diameter of the annulus cross section.

With all the assumptions and considerations given above the Young's modulus can be determined by

$$E = \frac{F H}{\pi d t \Delta H} \quad (22)$$

The numerical tests were performed with an approximate aspect ratio of $H/d = 21$. Consequently, the lengths of the investigated nanotubes range from 51.16 Å ((3,0), roll-up) up to 342.11 Å ((12,12), roll-up). This given aspect ratio ensures that the nanotube is long enough to reduce boundary effects. To be more precise, the evaluated length used to calculate the Young's modulus is not the whole nanotube length but a reduced length in the region of the nanotube where edge effects already decayed. This decay happens within the area of three unit cells from the nanotube ends for zig-zag nanotubes and six unit cells for armchair tubes, respectively. The edge effects are evaluated by comparing the deformed dimensions of a unit cell near the end with the deformed dimensions of one in the middle of the nanotube.

The mentioned modeling approaches and assumptions lead, when conducting a virtual tensile test with armchair and zig-zag carbon nanotubes, to the following results for the Young's modulus, see Fig. 10 and Tables 1 and 2.

Fig. 10 shows that the Young's modulus of small diameter armchair tubes is higher than the one of small diameter zig-zag tubes. For increasing diameters the values for the Young's modulus of the armchair and the zig-zag tubes converge to approximately 1 TPa which is also near the commonly accepted value of graphene. When comparing the results for both different geometric models used in this research, one can notice that the Young's modulus calculated on the basis of the roll-up model is larger than the one calculated using the exact polyhedral model, see Tables 1 and 2. It can also be observed that the deviation decreases with increasing diameters of the nanotubes. This is due to

the fact that when the diameter is increased, the geometry generated with the roll-up model matches the geometry of the exact polyhedral model better. Another difference can be recognized when comparing the progression of the Young's modulus of armchair tubes in dependence of the diameter for both geometrical models. The results for the Young's modulus based on the roll-up model basically show no dependence on the nanotube diameter at all. However, the results using the exact polyhedral model show a dependence on the diameter in terms of an increasing Young's modulus with increasing diameter. The reason for these deviations can solely be the usage of the two different geometric models and the therefore resulting geometrical deviations. These deviations include (i) differences in the bond lengths (roll-up model) and (ii) differences in the calculated nanotube diameters. These deviations are discussed in more detail in section 4.2.

In Fig. 11 a comparison between the results of the present research and some results available in literature is given. It can be observed, that all obtained values for the Young's modulus are ranged in the area of around 1 TPa. Differences can be recognized when having a closer look at the dependence of the Young's modulus with respect to the diameter. Some results show no or a weak dependence, while our results and the results computed by Tserpes and Papanikos (2005) show the already described dependence on the nanotubes diameter. This is an aspect in carbon nanotube research which is still under discussion. Furthermore it has to be noted that the deviations in the results for the Young's modulus are partly due to the circumstance that the results in literature are based on the roll-up geometric model. The results of the present research depicted in Fig. 11 are obtained by applying the exact polyhedral model.

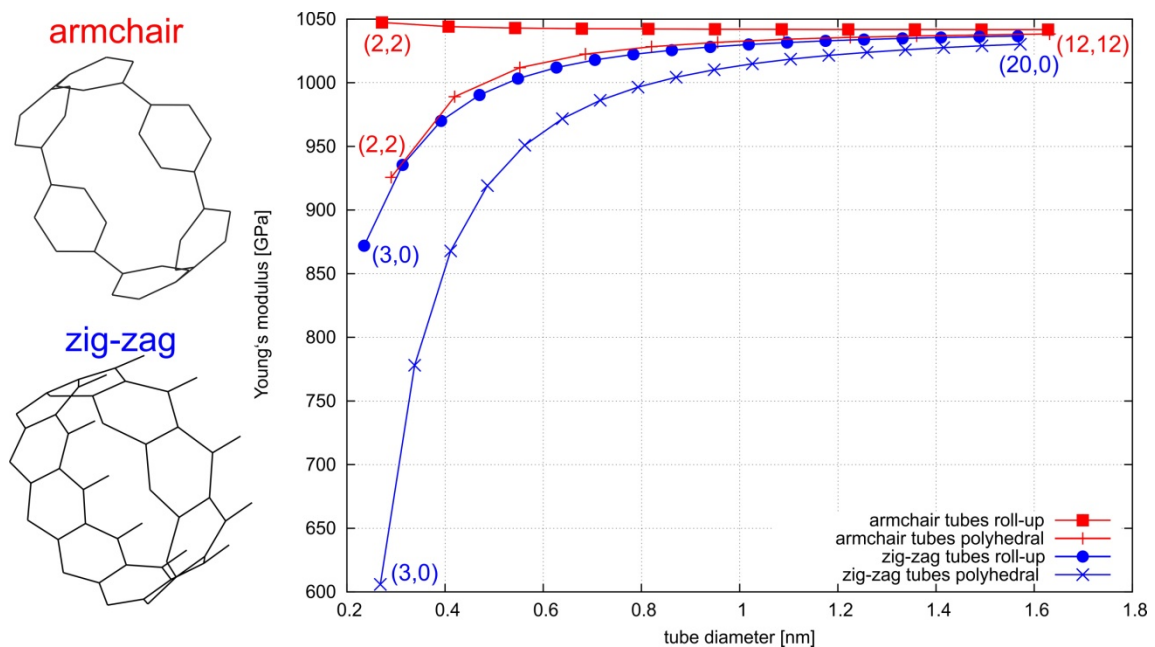


Fig. 10 Numerical results of the Young's modulus versus the nanotube diameter for armchair and zig-zag tubes when modeled with different geometrical approaches

Table 1 Results for Young's modulus of armchair SWCNTs

(n,m)	$d_{\text{roll-up}} [\text{\AA}]$	$d_{\text{polyhedral}} [\text{\AA}]$	$E_{\text{roll-up}} [\text{MPa}]$	$E_{\text{polyhedral}} [\text{MPa}]$	$\frac{ E_{\text{roll-up}} - E_{\text{polyhedral}} }{E_{\text{polyhedral}}} \cdot 100\%$
(2,2)	2.7139	2.9022	1 047 318	925 693	13.1
(3,3)	4.0709	4.1956	1 044 141	989 103	5.6
(4,4)	5.4278	5.5211	1 043 023	1 011 871	3.1
(5,5)	6.7848	6.8593	1 042 504	1 022 509	2.0
(6,6)	8.1417	8.2038	1 042 221	1 028 315	1.4
(7,7)	9.4987	9.5519	1 042 051	1 031 825	1.0
(8,8)	10.8556	10.9022	1 041 940	1 034 106	0.8
(9,9)	12.2126	12.2540	1 041 865	1 035 672	0.6
(10,10)	13.5696	13.6068	1 041 810	1 036 793	0.5
(11,11)	14.9265	14.9603	1 041 770	1 037 623	0.4
(12,12)	16.2835	16.3145	1 041 740	1 038 254	0.3

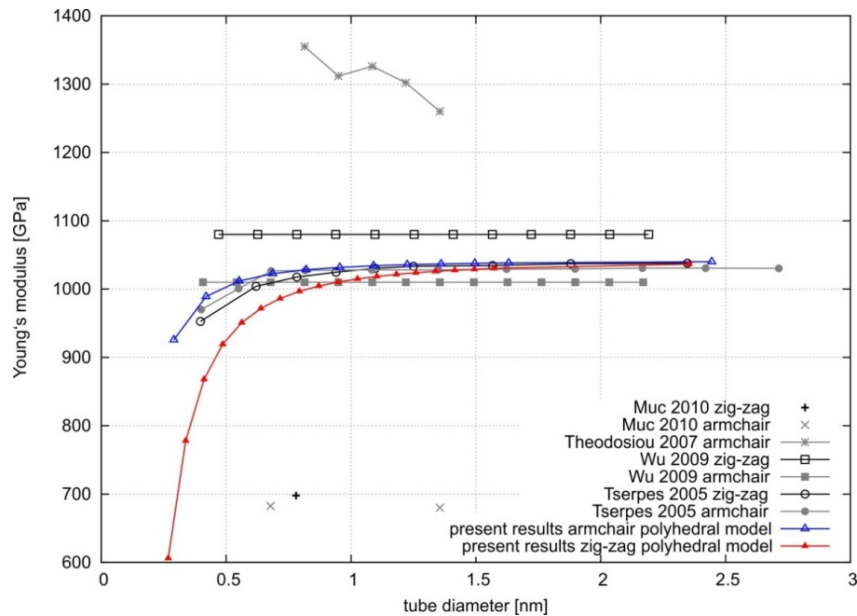


Fig. 11 Young's modulus versus nanotube diameter for armchair and zig-zag tubes. The results from the present research are based on the exact polyhedral model, the results given by other authors are based on the roll-up model with an assumed wall thickness of 0.34 nm. The results given here contain the works of Muc (2010), Theodosiou and Saravanos (2007), Wu *et al.* (2009) and Tserpes and Papanikos (2005)

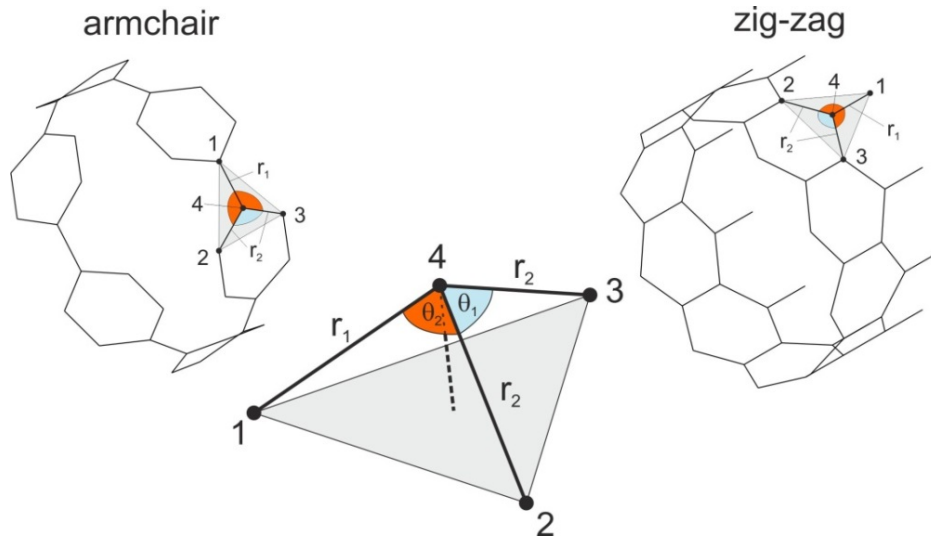


Fig. 12 Orientation of the tetrahedrons in the nanotube unit cells and their dimensions

4.2 Deformation behavior

In this section an attempt is made to identify the possible bond deformations in the carbon nanotube structure in order to get a better understanding of the deformation behavior of carbon nanotubes. It is useful to focus on a single tetrahedron inside the carbon nanotube. The reason for this is that it is possible to describe the deformation of the whole nanotube by the deformation of a single representative tetrahedron, see Fig. 12. This approach is shown in the present research by two different applications. The first one is the comparison of the results when using different geometrical models. The other application of this approach is to get a better understanding of the deformation mechanisms governing the mechanical behavior of carbon nanotubes.

Fig. 12 shows a representative tetrahedron in the unit cells of armchair and zig-zag carbon nanotubes. This figure also depicts the geometry of the tetrahedron, which is defined by the bond lengths and angles. The lengths are named r_1 and r_2 and the bond angles are θ_1 and θ_2 . It can be noticed that only two bond lengths and bond angles are distinguished. The explanation for this is that the nanotube deforms under tensile load in a way in which only two different values for the bond stretch and the bond angle occur. Furthermore, the curvature effects in tubes modeled with the roll-up geometric model lead to two different bond lengths in the undeformed state of armchair and zig-zag tubes. More details concerning the deformation behavior are given later in this section.

4.2.1 Comparison of the geometrical models

Regarding the comparison of nanotube properties when using different geometrical approaches, it is useful to focus at first on the properties of only one particular carbon nanotube, for instance, the (6, 0) zig-zag nanotube with a length of 25 unit cells. The nanotube is tested in a virtual tensile test and was subjected to 1% of tensile strain. When comparing the results for the Young's modulus

of this tube, see Table 3, it can be seen that the Young's modulus for the tube modeled with the roll-up model is higher than the Young's modulus for the one modeled with the exact polyhedral model. This difference can be explained with a closer look at the dimensions of the undeformed tetrahedron in the nanotubes as it is given in Table 3. In this table, a difference in the bond lengths r_1 and r_2 in the undeformed state of the nanotube when using the roll-up model is shown. As already shown in section 3.1, the occurrence of unequal bond lengths is an undesired effect of the roll-up model as a result of the improperly accounted curvature during the rolling of the graphene sheet. The same problem can be observed when comparing the bond angles θ_1 and θ_2 in the undeformed state of the tube using the roll-up model. The exact polyhedral model doesn't show this issue, since it computes equal bond lengths and angles. The unequal dimensions occurring in the roll-up model result in a different load distribution inside the nanotube when compared to the exact polyhedral model and hence in the deviation of the values for the Young's modulus. For larger diameters the geometrical deviations decrease and also the differences in the Young's modulus become smaller. As example for this effect refer to Table 4, where the undeformed dimensions of a (6, 6) armchair SWCNT with a length of 70 unit cells are given. Compared to the (6, 0) zig-zag tube, the (6, 6) armchair tube has a larger diameter resulting in smaller deviations between the roll-up and the exact polyhedral model.

Table 2 Results for Young's modulus of zig-zag SWCNTs

(n,m)	$d_{\text{roll-up}} [\text{\AA}]$	$d_{\text{polyhedral}} [\text{\AA}]$	$E_{\text{roll-up}} [\text{MPa}]$	$E_{\text{polyhedral}} [\text{MPa}]$	$\frac{ E_{\text{roll-up}} - E_{\text{polyhedral}} }{E_{\text{polyhedral}}} \cdot 100\%$
(3,0)	2.3503	2.6795	871 930	605 892	43.9
(4,0)	3.1338	3.3797	935 472	778 011	20.2
(5,0)	3.9172	4.1130	970 011	867 866	11.8
(6,0)	4.7006	4.8632	990 389	919 155	7.7
(7,0)	5.4841	5.6231	1 003 280	950 872	5.5
(8,0)	6.2675	6.3890	1 011 904	971 762	4.1
(9,0)	7.0509	7.1588	1 017 937	986 219	3.2
(10,0)	7.8344	7.9314	1 022 315	996 625	2.6
(11,0)	8.6178	8.7060	1 025 587	1 004 359	2.1
(12,0)	9.4013	9.4820	1 028 096	1 010 260	1.8
(13,0)	10.1847	10.2592	1 030 060	1 014 865	1.5
(14,0)	10.9681	11.0373	1 031 626	1 018 525	1.3
(15,0)	11.7516	11.8161	1 032 894	1 021 483	1.1
(16,0)	12.5350	12.5955	1 033 935	1 023 907	1.0
(17,0)	13.3185	13.3754	1 034 800	1 025 918	0.9
(18,0)	14.1019	14.1556	1 035 527	1 027 604	0.8
(19,0)	14.8853	14.9363	1 036 142	1 029 032	0.7
(20,0)	15.6688	15.7171	1 036 669	1 030 252	0.6

Table 3 Undeformed dimensions of a representative tetrahedron in a (6, 0) zig-zag tube

undeformed state	roll-up	exact polyhedral	$\frac{ X_{\text{roll-up}} - X_{\text{polyhedral}} }{X_{\text{polyhedral}}} \cdot 100\%$
r_1 [nm]	0.142100	0.142100	0
r_2 [nm]	0.140888	0.142100	0.86
θ_1 [°]	113.05	117.65	4.07
θ_2 [°]	120.28	117.65	2.19
E [MPa]	990 389	919 155	7.70

4.2.2 Investigation of bond deformation in armchair and zig-zag nanotubes

Besides the investigation of the two presented geometrical models the understanding of the deformation mechanisms of the carbon nanotubes is another interesting topic. The basic question to deal with in this context is how the deformed tube arises from the original configuration. To get a deeper understanding of this it is necessary to look at the unit cells in the nanotubes and in particular to focus on the deformations of each single covalent bond. At this level it is possible to distinguish the bond deformations into the three types mentioned before, namely the

- bond stretching,
- bond angle bending and the
- bond torsion.

Hence, it was investigated in which bonds of the armchair and zig-zag tubes the mentioned bond deformations occur. An overview on the deformations in the unit cell of armchair and zig-zag nanotubes is given in Fig. 13. Even though the figure depicts a (6, 6) armchair and a (10, 0) zig-zag unit cell, the considerations made in this section are valid for arbitrary armchair and zig-zag nanotubes. A more detailed view of the bond stretching and bond angle bending of the investigated tubes is given in Fig. 14. In the following, the possible bond deformations are analyzed and described in detail.

Table 4 Undeformed dimensions of a representative tetrahedron in a (6, 6) armchair tube

undeformed state	roll-up	exact polyhedral	$\frac{ X_{\text{roll-up}} - X_{\text{polyhedral}} }{X_{\text{polyhedral}}} \cdot 100\%$
r_1 [nm]	0.141380	0.142100	0.51
r_2 [nm]	0.142055	0.142100	0.03
θ_1 [°]	120.06	119.24	0.68
θ_2 [°]	118.85	119.24	0.33
E [MPa]	1 042 221	1 028 315	1.4

Bond stretching: Bond stretching can be found in both, armchair and zig-zag nanotubes. However, the armchair and the zig-zag tubes show a different behavior of the bond stretching.

Starting with the armchair tubes, a stretching can be noticed only in the covalent bonds which are not perpendicular to the nanotube axis (blue color), see Fig. 13 (left). For a closer look of the bond stretch behavior, the original bond lengths given in Fig. 14(a) are used as starting point. With this geometry in mind it is possible to extract from Fig. 14(c) that the blue colored bonds with the original length r_2 both show the same extension Δr_2 of the bond. The black colored bonds with the original bond length r_1 show no bond stretching at all.

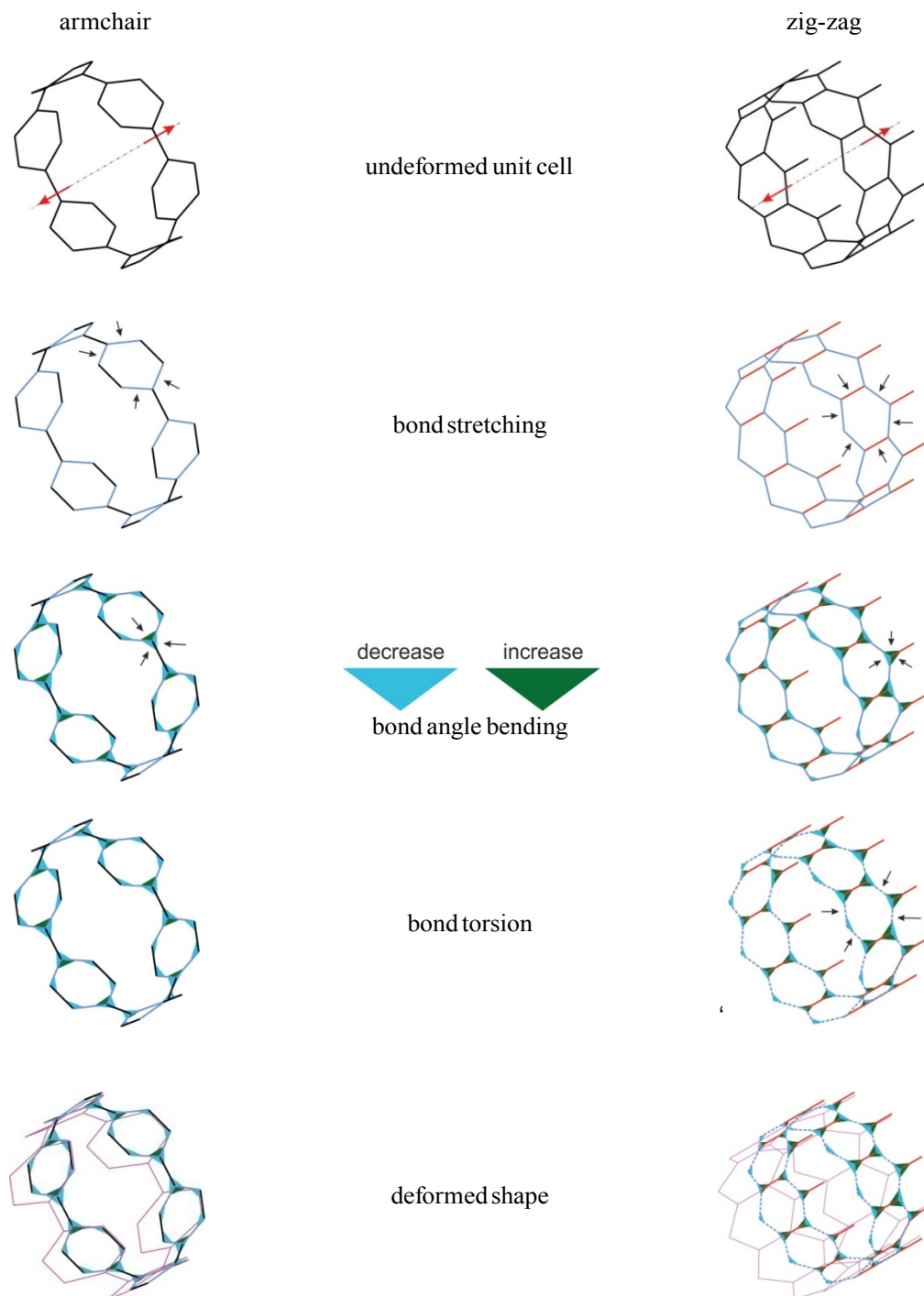


Fig. 13 Deformation mechanisms in armchair and zig-zag carbon nanotubes. The red arrows in the undeformed unit cell indicate the direction of the tensile test

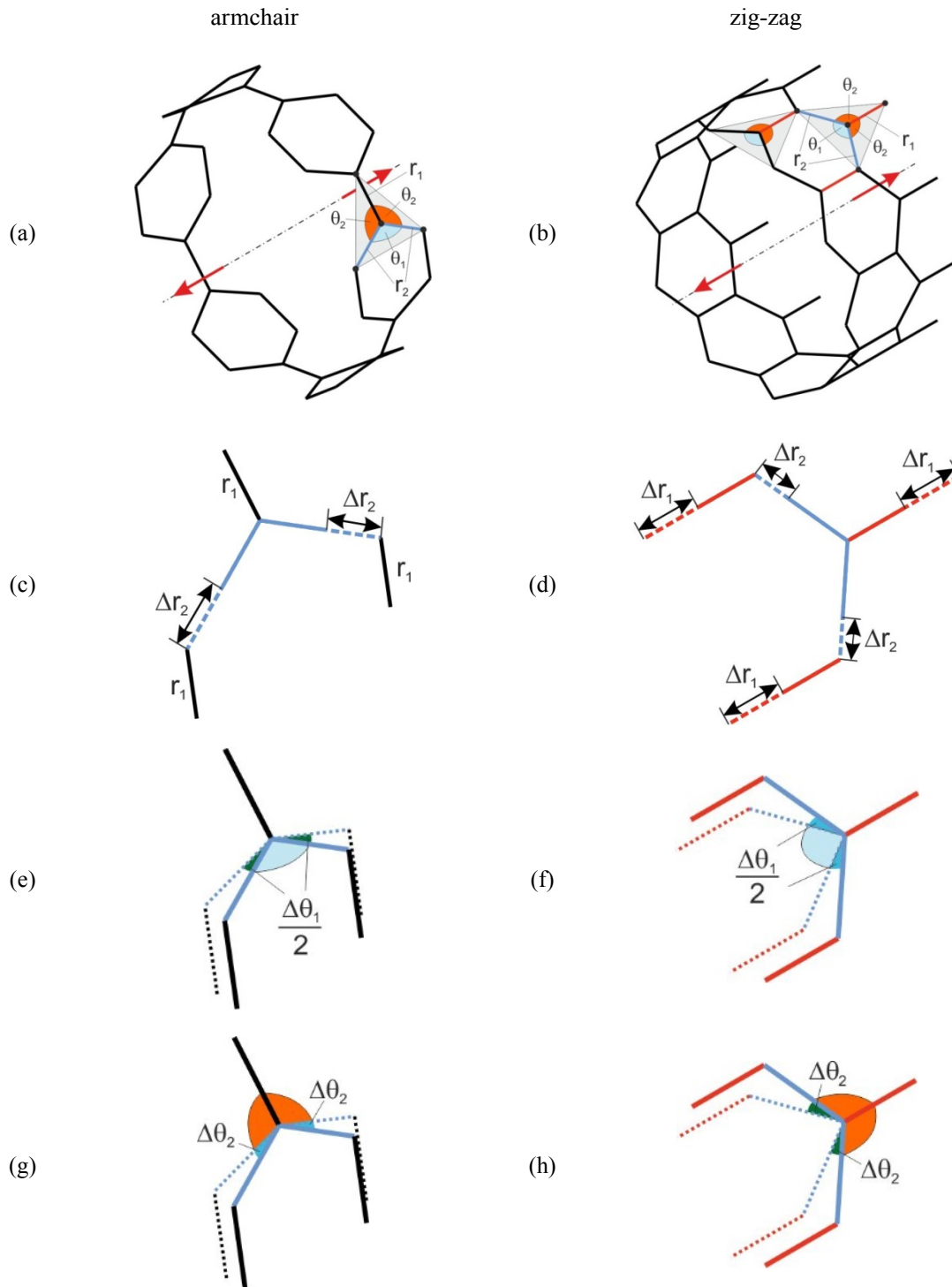


Fig. 14 Detailed view at the deformations occurring in armchair and zig-zag carbon nanotubes. The deformed configuration is represented by dotted lines

In the zig-zag nanotubes all the bonds show an extension. Again, the original bond lengths are given in Fig. 14(b). In these tubes two different values for the tube extension can be distinguished (blue and red colored), see Fig. 14(d). Here, the red bonds in the direction of the nanotube show larger bond extensions Δr_1 than the blue bonds, in which a bond extension of Δr_2 can be observed.

Bond angle bending: Bond angle bending can be found in both investigated nanotube types. In Fig. 13, a decrease of the bond angle is depicted with a blue colored triangle, while an increase is shown by a green triangle. For armchair and zig-zag type SWCNTs two different bond angle changes can be observed.

Concerning the behavior of the armchair tubes, the considerations again start by looking at the original dimensions of the bond angles which are given in Fig. 14(a). As it can be observed in Fig. 13, two different bond angle changes have to be taken into account. These bond angle changes are given in detail in Figs. 14(e) and 14(g). Here, an increase of the angle θ_1 and a decrease of the two angles θ_2 is observed. It has to be noted that the increase of θ_1 is not equal to the decrease of the two θ_2 angles since the tetrahedron where these angles are defined in, is a spatial structure.

Regarding the zig-zag nanotubes, the original dimensions are given in Fig. 14(b). Analogous to the armchair tubes, the zig-zag tubes show two different bond angle changes. From Figs. 14(f) and 14(h) a decrease of the angle θ_1 and an increase of the angles θ_2 can be extracted. Due to the reasons given above, the decrease and the increase of the corresponding angles are not equal.

Bond torsion: Armchair tubes do not show any bond torsion at all. In zig-zag tubes it is possible to observe bond torsion in the blue colored dotted bonds. These are the bonds which are not orientated in the direction of the tube axis.

The geometry of the representative tetrahedron is defined by the bond lengths and bond angles only. Within this research it is assumed that bond torsion affects the bond angle change. This is the reason why no separate detail figures for the bond torsion are given in Fig. 14.

Fig. 13 also shows the deformed shape of the unit cell, when the whole carbon nanotube is subjected to a tensile force.

Tables 5 and 6 present the deformed dimensions of representative tetrahedrons in a (6,0) zig-zag and a (6,6) armchair tube. For comparison with the undeformed dimensions please refer to Tables 3 and 4. The conclusions given in this section are valid for the whole investigated unit cell. Furthermore, they are valid for every unit cell of the nanotube with a sufficient distance from the nanotube ends where edge effects already decayed. Estimated reference values for this distance are six unit cells for armchair and three unit cells for zig-zag nanotubes.

Table 5 Deformed dimensions of a representative tetrahedron in a (6, 0) zig-zag tube

deformed state	roll-up	exact polyhedral	$\frac{ X_{\text{roll-up}} - X_{\text{polyhedral}} }{X_{\text{polyhedral}}} \cdot 100\%$
r_1 [nm]	0.143371	0.143320	0.04
r_2 [nm]	0.141208	0.142386	0.83
θ_1 [°]	112.46	117.08	3.95
θ_2 [°]	120.61	117.98	2.23

Table 6 Deformed dimensions of a representative tetrahedron in a (6, 6) armchair tube

deformed state	roll-up	exact polyhedral	$\frac{ X_{\text{roll-up}} - X_{\text{polyhedral}} }{X_{\text{polyhedral}}} \cdot 100\%$
r_1 [nm]	0.141380	0.142100	0.51
r_2 [nm]	0.143060	0.143095	0.02
θ_1 [°]	120.64	119.83	0.68
θ_2 [°]	118.57	118.96	0.33

4. Conclusions

In the present research a molecular mechanics approach was applied to single wall carbon nanotubes (SWCNTs) in order to (i) calculate their mechanical properties (Young's modulus) and to (ii) provide a deeper understanding of the governing deformation mechanisms.

In the molecular mechanics approach two different issues were taken into account: (i) the nanotube geometry and (ii) the representation of the covalent bonds. Regarding the nanotube geometry, two different geometrical models, the roll-up and the exact polyhedral model according to Cox and Hill were applied. The bond representation was based on the molecular structural mechanics approach by Li and Chou. A virtual tensile test was conducted for several armchair and zig-zag nanotubes with different diameters. Beside the main targets mentioned above, the numerical simulation was used to illuminate the deviations arising from the application of the different geometrical models. Regarding these topics of the present research, the following conclusions can be drawn:

Young's modulus

- The Young's modulus calculated in the present research is in excellent agreement with results available in literature.
- The dependence of the Young's modulus versus the diameter still needs further investigation since the results available in literature show different progressions.
- The calculation of a stiffness instead of the Young's modulus is proposed in order to avoid assumptions which cannot be conciliated with physical basics.

Comparison of the geometrical models

- When comparing the results of the Young's modulus calculated with the two different applied models, one can observe that:
 - Nanotubes modeled with the roll-up model show a higher Young's modulus than the nanotubes based on the exact polyhedral model.
 - Armchair tubes show a different dependence of the Young's modulus versus the diameter for the different applied geometrical models.
 - The deviations arising when different geometrical models are applied decrease for increasing nanotube diameters.

Investigation of bond deformation in armchair and zig-zag nanotubes

- The decomposition of the nanotube deformation into the contributions stemming from each individual bond provides a deeper insight into the deformation mechanisms of carbon nanotubes.

In further research an enhanced decomposition of the nanotube deformations will be investigated, in which the role of the bond torsion is illuminated in more detail. After the clarification of the bond torsion influence, other load cases besides tensile loading will be investigated in order to extend the understanding of the deformation behavior of carbon nanotubes.

Acknowledgements

This research has been sponsored by the Deutsche Forschungsgemeinschaft (DFG) within the grant WA2323/6-1.

References

- Baughman, R.H., Cui, C., Zakhidov, A.A., Iqbal, Z., Barisci, J.N., Spinks, G.M., Wallace, G.G., Mazzoldi, A., De Rossi, D., Rinzler, A.G., Jaschinski, O., Roth, S. and Kertesz, M. (1999), "Carbon nanotube actuators", *Science*, **284**(5418), 1340-1344.
- Berber, S., Kwon, Y.K. and Tománek, D. (2000), "Unusually high thermal conductivity of carbon nanotubes", *Phys. Rev. Lett.*, **84**, 4613-4616.
- Chandraseker, K. and Mukherjee, S. (2007), "Atomistic-continuum and ab initio estimation of the elastic moduli of single-walled carbon nanotubes", *Comput. Mater. Sci.*, **40**(1), 147-158.
- Chen, W.H., Cheng, H.C. and Liu, Y.L. (2010), "Radial mechanical properties of single-walled carbon nanotubes using modified molecular structure mechanics", *Comput. Mater. Sci.*, **47**(4), 985-993.
- Cinefra, M., Carrera, E. and Brischetto, S. (2011), "Refined shell models for the vibration analysis of multi-walled carbon nanotubes", *Mech. Adv. Mater. Str.*, **18**(7), 476-483.
- Cornell, W.D., Cieplak, P., Bayly, C.I., Gould, I.R., Merz, K.M., Ferguson, D.M., Spellmeyer, D.C., Fox, T., Caldwell, J.W. and Kollman, P.A. (1995), "A second generation force field for the simulation of proteins, nucleic acids, and organic molecules", *J. Am. Chem. Soc.*, **117**(19), 5179-5197.
- Cox, B.J. and Hill, J.M. (2007), "Exact and approximate geometric parameters for carbon nanotubes incorporating curvature", *Carbon*, **45**(7), 1453 - 1462.
- Dresselhaus, M., Dresselhaus, G. and Saito, R. (1995), "Physics of carbon nanotubes", *Carbon*, **33**(7), 883-891.
- Foroughi, J., Spinks, G.M., Wallace, G.G., Oh, J., Kozlov, M.E., Fang, S., Mirfakhrai, T., Madden, J.D.W., Shin, M.K., Kim, S.J. and Baughman, R.H. (2011), "Torsional carbon nanotube artificial muscles", *Science*, **334**(6055), 494-497.
- Giannopoulos, G., Kakavas, P. and Anifantis, N. (2008), "Evaluation of the effective mechanical properties of single walled carbon nanotubes using a spring based finite element approach", *Comput. Mater. Sci.*, **41**(4), 561 - 569.
- Hernández, E., Goze, C., Bernier, P. and Rubio, A. (1998), "Elastic properties of C and $B_xC_y N_z$ composite nanotubes", *Phys. Rev. Lett.*, **80**(20), 4502-4505.
- Iijima, S. (1991), "Helical microtubules of graphitic carbon", *Nature*, **354**, 56.
- Iijima, S. and Ichihashi, T. (1993), "Single-shell carbon nanotubes of 1-nm diameter", *Nature*, **363**, 603-605.
- Kudin, K.N., Scuseria, G.E. and Yakobson, B.I. (2001), " C_2F , BN, and C nanoshell elasticity from *ab initio*

- computations”, *Phys. Rev. B.*, **64**(23), 235406.
- Li, C. and Chou, T.W. (2003), “A structural mechanics approach for the analysis of carbon nanotubes”, *Int. J. Solids Struct.*, **40**(10), 2487-2499.
- Lu, W., Zu, M., Byun, J.H., Kim, B.S. and Chou, T.W. (2012), “State of the art of carbon nanotube fibers: opportunities and challenges”, *Adv. Mater.*, **24**(14), 1805-1833.
- Meo, M. and Rossi, M. (2006), “Prediction of Young’s modulus of single wall carbon nanotubes by molecular- mechanics based finite element modelling”, *Compos. Sci. Technol.*, **66**(11-12), 1597-1605.
- Muc, A. (2010), “Design and identification methods of effective mechanical properties for carbon nanotubes”, *Mater. Design*, **31**(4), 1671-1675.
- Odegard, G.M., Gates, T.S., Nicholson, L.M. and Wise, K.E. (2002), “Equivalent-continuum modeling of nano-structured materials”, *Compos. Sci. Technol.*, **62**, 1869-1880.
- Radushkevich, L.V. and Lukyanovich, V.M. (1952), “About the structure of carbon formed by thermal decomposition of carbon monoxide on iron substrate”, *J. Phys. Chem.(Moscow)*, **26**, 88-95.
- Sánchez-Portal, D., Artacho, E., Soler, J.M., Rubio, A. and Ordejón, P. (1999), “Ab initio structural, elastic, and vibrational properties of carbon nanotubes”, *Phys. Rev. B*, **59**(19), 12678-12688.
- Tans, S.J., Devoret, M.H., Dai, H., Thess, A., Smalley, R.E., Geerligs, L.J. and Dekker, C. (1997), “Individual single-wall carbon nanotubes as quantum wires”, *Nature*, **386**, 474-477.
- Theodosiou, T. and Saravanos, D. (2007), “Molecular mechanics based finite element for carbon nanotube modeling”, *Comput. Model. Eng. Sci.*, **19**(2), 121-134.
- Thostenson, E.T., Ren, Z. and Chou, T.W. (2001), “Advances in the science and technology of carbon nanotubes and their composites: a review”, *Compos. Sci. Technol.*, **61**(13), 1899 -1912.
- Treacy, M.M.J., Ebbesen, T.W. and Gibson, J.M. (1996), “Exceptionally high Young’s modulus observed for individual carbon nanotubes”, *Nature*, **381**, 678- 680.
- Tserpes, K. and Papanikos, P. (2005), “Finite element modeling of single-walled carbon nanotubes”, *Compos. Part B.*, **36**(5), 468-477.
- Wu, C.J., Chou, C.Y., Han, C.N. and Chiang, K.N. (2009), “Estimation and validation of elastic modulus of carbon nanotubes using nano-scale tensile and vibrational analysis”, *Comput. Model. Eng. Sci.*, **41**(1), 49-67.
- Wu, Y., Huang, M., Wang, F., Huang, X.M.H., Rosenblatt, S., Huang, L., Yan, H., O’Brien, S.P., Hone, J. and Heinz, T.F. (2008), “Determination of the Young’s modulus of structurally defined carbon nanotubes”, *Nano Lett.*, **8**(12), 4158-4161.